Laser-seeded modulation instability within LHC proton beams

Carl Siemon, Vladimir Khudik, S. Austin Yi, Alexander Pukhov, and Gennady Shvets

Citation: AIP Conference Proceedings **1507**, 629 (2012); doi: 10.1063/1.4773770
View online: http://dx.doi.org/10.1063/1.4773770
View Table of Contents: http://scitation.aip.org/content/aip/proceeding/aipcp/1507?ver=pdfcov
Published by the AIP Publishing

Laser-seeded modulation instability within LHC proton beams

Carl Siemon*, Vladimir Khudik*, S. Austin Yi*, Alexander Pukhov† and Gennady Shvets*

*The University of Texas at Austin, Austin, Texas 78712
†Max-Planck-Institut für Physik, 80805 München, Germany

Abstract. A new method for seeding the modulation instability (MI) within an SPS-LHC proton beam using a laser pulse is presented. Using simulations, we show that a laser pulse placed ahead of a proton beam excites axially symmetric self-modulation modes within the proton beam and leads to peak accelerating fields that are comparable to previously proposed seeding methods.

Keywords: Proton driven wakefield acceleration
PACS: 29.27.-a

INTRODUCTION

In the past decade, plasma based particle acceleration has made considerable advances. 10-100 GeV electrons have been reported using either laser or particle beams as the driver [1]. To achieve higher electron energies with a laser driver, improvements in power, focusing, and repetition rate are required. In particle-beam driven acceleration, the maximum energy gain of the witness bunch is restricted by the transformer ratio limit, which roughly states that a witness bunch's energy cannot exceed the driver bunch's energy [2].

To achieve unprecedented electron beam energies in the TeV range, TeV proton beams from CERN's Large Hadron Collider (LHC) have been proposed as a driver for plasma based particle acceleration [3]. In order to efficiently excite plasma waves that produce large accelerating gradients, the driver beam should be of order one plasma wavelength, $\lambda_p \sim 2\pi c/\omega_p$, where $\omega_p = \sqrt{\frac{4\pi e^2 n_{p0}}{m_e}}$ is the plasma frequency, c is the speed of light, n_{p0} is the unperturbed plasma number density, e is electron charge, and m_e is the electron mass. However, suggested plasma wavelengths of order 1 mm, which corresponds to the wave-breaking field of $\sim$1 GV/m, are much shorter than the r.m.s length of the proton beams at the LHC, $\sigma_z \sim 100\ \lambda_p$.

To resonantly excite plasma waves using a long proton beam, it has been suggested to rely on the so-called modulation instability (MI) within the proton beam to separate the beam into a 'train' of bunchlets of length $\sim \lambda_p/2$ separated by λ_p [4, 5]. The MI is a parametric, transverse, and axially symmetric electro-magnetic instability. It arises within long beams with $\sigma_z >> \lambda_p$ and occurs because the beam generates its own wakefield within its body, leading to its self modulation and stronger wakefields, forming a positive feedback loop. The electrostatic, longitudinal two-stream instability [6] is expected to not play a dominent role in relativistic LHC beams because this instability develops from the longitudinal displacement of beam particles with respect to each other, which cannot happen if all particles' velocity remains close to c. The transverse electro-magnetic Weibel Instability [7], which is dominent for long, wide, and relativistic beams and leads to the formation of beam filaments of r.m.s transverse width $\sigma_r \sim c/\omega_p$, cannot develop in LHC beams since their σ_r is initially $\sim c/\omega_p$.

The 'hosing-instability' (HI) [8], which develops in essentially the same way as the MI, but results in non-axially symmetric modulation throughout the proton beam, can also play an important role in the beam's evolution if given time to develop. Due to the HI's assymetric nature, wakefield contributions from preceding protons do not add in a coherent manner, so that the wakefields and accelerating gradients are much smaller than in the case of the MI. To excite axially symmetric instability modes within the beam and ensure that the MI develops without the presence of the HI, the most popular proposed, but not currently experimentally feasible seeding method, is to 'hard cut' the proton beam in the longitudinal direction using a 'dog-leg' device [5]. This creates a very sharp and large transition in beam density at the beam's head. For a quiescent, quasi-neutral plasma, this excites a considerable plasma electron number density perturbation $\delta n_p \sim n_{b0}$ throughout the proton beam, where n_{b0} is the initial, maximum number density of the

Advanced Accelerator Concepts
AIP Conf. Proc. 1507, 629-633 (2012); doi: 10.1063/1.4773770

beam. This perturbation efficiently excites the MI before the HI has time to develop.

In this proceedings paper, we demonstrate that a laser pulse placed ahead of an LHC proton bunch can efficiently seed the MI and create maximal accelerating gradients that are comparable to the hard-cut seeding method. To accomplish this, we report simulation results for the following scenarios: a laser pulse with non-stringent parameters is placed in front of a proton beam with initial density profile

$$n_b = \frac{n_{b0}}{2} \exp\left(-r^2/\sigma_r^2\right)[1+\cos[\sqrt{\frac{\pi}{2}}\frac{(\zeta-\sigma_z\sqrt{2\pi})}{\sigma_z}]] \tag{1}$$

for $0 < \zeta < 2\sigma_z\sqrt{2\pi}$, where $\zeta = ct - z$ is the proton beam's co-moving coordinate; the same beam is hard-cut without a laser-pulse. Note that others [5, 11] use $\exp\left(-r^2/(2\sigma_r^2)\right)$ instead for the radial dependence in this expression.

SIMULATION MODEL

We begin with a brief description of the simulation model used to generate the results reported in this paper. The beam's protons are treated kinetically, plasma ions immobile, and plasma electrons as a fluid. The plasma response is assumed to be linear, so that

$$\frac{\partial^2 \delta n_p}{\partial \zeta^2} + k_p^2 \delta n_p = k_p^2 n_b + n_{p0}\nabla^2\left(\frac{|a|^2}{4}\right), \tag{2}$$

where $\zeta = ct - z$ is the co-moving longitudinal coordinate, $k_p = \omega_p/c = \sqrt{4\pi e^2 n_{p0}/m_e c^2}$, $|a| = \frac{e}{mc\omega_0}|\vec{E}_L|$ is the laser's normalized magnetic vector potential, ω_0 is the laser's angular frequency, and $\vec{E}_L$ is the laser's electric field. Note that the response of the plasma is equivalent to that of a harmonic oscillator driven by the beam and laser pulse. The linear approximation is justified for underdense proton beams, weakly to mildly relativistic laser parameters, and modest beam-lengths, which are consistent with those used in this paper. For longer proton beams, it is possible for plasma density waves induced by the proton beam to superimpose and cause $\delta n_p/n_{p0} \sim 1$ to be satisfied in selected regions, even though $n_b << n_{p0}$. σ_z is therefore chosen to ensure that the linear model remains valid throughout the proton beam's evolution, which restricts us to beam lengths that are roughly 2-3 times shorter than the SPS-LHC σ_z of 12 cm. However, our demonstration of the laser-seeded MI using these shorter beams is still valid as a proof a principle.

The laser is evolved according to the solution for a diffracting Gaussian pulse in vacuum: $w(z) = w_0\sqrt{1+z^2/z_R^2}$,

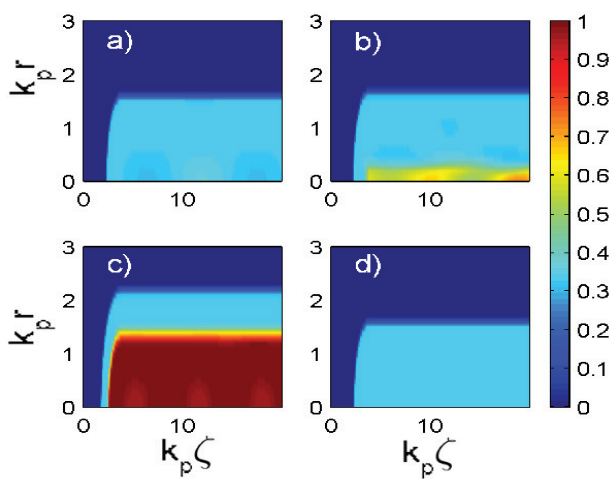

FIGURE 1. Ionization level n_{p0}/n_{p0}^{max} of Cesium vapor for different laser parameters. (a), (b), (c), (d)- $a_0 = .15$, $a_0 = .2$ for $\lambda_L = 10$ μm laser and $a_0 = .15$, $a_0 = .015$ for $\lambda_L = 1$ μm laser, respectively. Light blue regions correspond to first level ionization while green, yellow, and red regions correspond to secondary and tertiary ionization. Laser pulse is at $k_p\zeta = 4$ and has r.m.s length and width of k_p^{-1}.

where $w(z)$ is the pulse's waist size as a function of propagation distance z, w_0 is $w(z)$ at the beam's focal plane located at $z = 0$, $z_R = \pi w_0^2/\lambda_L$ is the Rayleigh range, and λ_L is the laser's wavelength. $|a|$ is calculated from $w(z)$ according to $|a|^2 = a_0^2(w_0/w(z))^2 e^{-2r^2/w(z)^2} e^{-\zeta^2/(\sigma_z^L)^2}$, where a_0 is the maximum value of $|a|$ at $z = 0$, σ_z^L is the pulse's longitudinal r.ms. length, and r is the transverse radial coordinate. For a laser with $a_0 = .1$, $w_0 \sim \sigma_z^L \sim 200$ μm, and $\lambda_L = 10$ μm, this treatment is a valid approximation since $w_0, \sigma_z^L << \lambda_L$ and the corresponding laser power $\frac{\pi}{2} w_0^2 (a_0/.85)^2 (1\mu m/\lambda_L)^2 10^{18}$ W/c.m$^2 \sim 1$ GW is much smaller than the critical power for relativistic self-focusing, $P_{crit} = (16.2 \text{ GW}) \times \omega_0^2/\omega_p^2 \sim .3$ PW .

We note that it is possible for the laser pulse to ionize the second level of Cesium vapor, which is the plasma source for the planned SPS-LHC experiments. This is undesirable since secondary ionization will increase n_{p0} when the laser is present. Figure 1 shows the ionization level n_{p0}/n_{p0}^{max} of Cesium vapor calculated using the ADK model [10] for different laser parameters, where $n_{p0}^{max} = 2.1 \cdot 10^{15}$ c.m^{-3} is the maximum n_{p0} value considering only the first three ionization levels of Cesium. Without any secondary or tertiary ionization, one hundred percent ionization of the first level of Cesium corresponds to $n_{p0} = 7 \cdot 10^{14}$ c.m^{-3}, the number density for the planned SPS-LHC experiments. k_p is calculated from this value throughout the paper. The figure shows that for a laser with $\lambda_L = 10$ μm, a_0 values above .2 (intensities greater than $\sim 5.5 \cdot 10^{14}$ W/c.m^2) produce significant secondary ionization. The figure also demonstrates that for a $\lambda_L = 1$ μm laser, significantly lower a_0 values produce secondary and tertiary ionization. A CO_2 laser with $\lambda_L \sim 10$ μm is therefore a more attractive candidate to seed the MI, so we take $\lambda_L = 10$ μm and $a_0 = .1$ in most of our simulations, although higher a_0 values are used for demonstration purposes in the final section of this paper.

The proton beam's relativistic $\gamma = 1/\sqrt{1-\beta_0^2}$ factor is assumed to be constant and ultra-relativistic ($\gamma >> 1$), where $\beta_0 = v_{bz}/c$ is the beam's normalized longitudinal velocity in the laboratory frame, so that only their transverse momenta and positions are evolved in a computational 'window' co-propagating with the beam. The beam's response is connected to that of the plasma through the transverse equation of motion for the i^{th} proton-

$$\frac{d(\gamma m v_\perp^i)}{dt} = F_\perp^i, \tag{3}$$

where $\vec{F}_\perp = e\vec{W}_\perp = e\vec{E}_\perp + e\hat{z} \times \vec{B}_\perp$ is the transverse force exerted by the plasma wakefield $\vec{W}_\perp$ on the proton and $v_\perp$ is its transverse velocity. The wakefield and longitudinal electric field E_z are determined from the equation

$$(\nabla_\perp^2 - k_p^2)\psi = -4\pi e \delta n_p, \tag{4}$$

where

$$E_z = -\partial_\zeta \psi, \tag{5}$$

$\vec{W}_\perp = \vec{\nabla}_\perp \psi$ [9], and ψ is the z component of the magnetic vector potential subtracted from the electrostatic potential.

LASER-SEEDED MODULATION INSTABILITY

Next, a qualitative description is given that explains how the laser pulse seeds the MI. Throughout this paper, the laser parameters $w_0 = \sigma_z^L = k_p^{-1}$ are used, which were found to most efficiently seed the MI for a proton beam with $\sigma_r = k_p^{-1} = 200$ μm (consistent with SPS-LHC parameters). For the proton beam parameters used throughout this paper, the corresponding diffraction distance z_R of a $\lambda_L = 10$ μm laser is much smaller than $c/\omega_\beta = c\sqrt{\frac{\gamma m_p}{4\pi e^2 n_{b0}}}$, where ω_β is the betatron frequency of the proton beam. Since c/ω_β is the propagation distance over which the MI develops, this implies that the laser's wakefield cannot directly drive the MI for a long enough distance. In order to efficiently seed the MI, the laser's wakefield must exert a force that produces a large, radially inward momentum in regions of the proton beam separated by $\sim \lambda_p$. This leads to the eventual compression of the proton beam in these regions after the laser has diffracted away, which provides a sinusoidal perturbation in beam density that seeds the MI.

We now present simulation results that demonstrate efficient excitation of the MI using a laser pulse seed. The proton beam has an initial density profile given by Eq. (1). The proton beam parameters used are $n_{b0}/n_{p0} = 1/500$, $\sigma_r = k_p^{-1}$, $\sigma_z = 3.8$ cm, angular divergence $\sigma_\theta = .04$ mrad, and energy 450 GeV. The beam's betatron length c/ω_β is 4.2 meters and $z_R = .013$ meters. The plasma density, which is used throughout this paper, is $n_{p0} = 7 \cdot 10^{14}$ c.m^{-3}, which corresponds to $\lambda_p = 1.3$ mm. With the exception of σ_z, these match the parameters of the planned SPS-LHC experiment. The center of the laser pulse is placed at location $\zeta = 0$, where the beam density is zero. This is shown

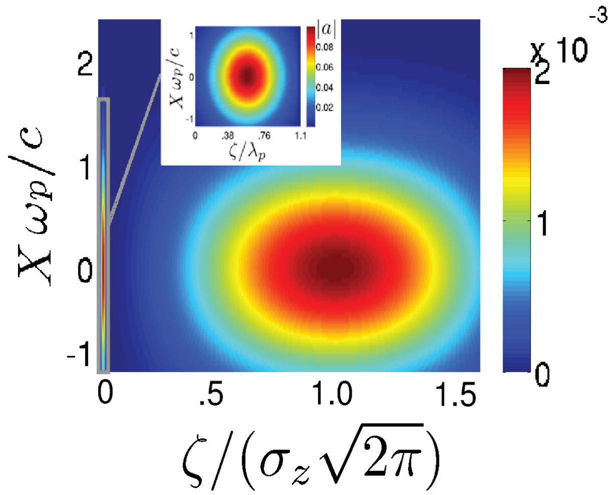

FIGURE 2. Schematic showing centered line-outs of n_b/n_{p0} (main picture) and $|a|^2$ (inset) as a function of ζ at initial simulation time. X represents the distance from the center of the beam.

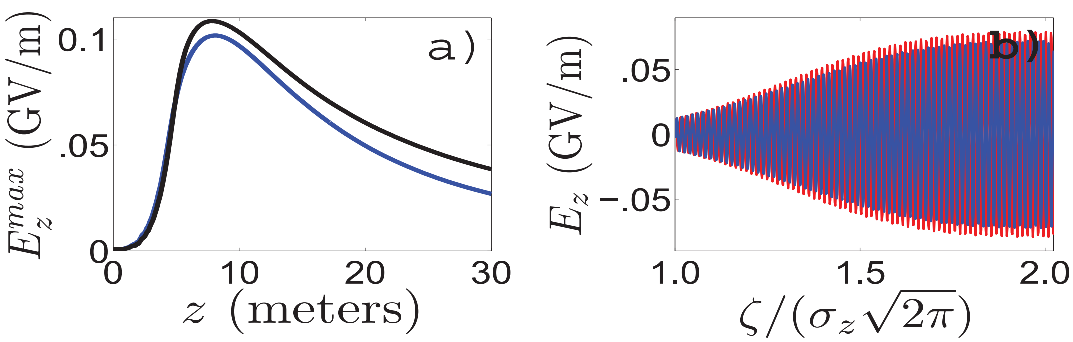

FIGURE 3. Simulation of laser-seeded modulation instability. (a)- Simulated E_z^{max} vs. z for proton beam hard-cut at $\zeta = \sigma_z\sqrt{\pi/2}$ with no laser (black line) and for the 'full' proton beam with a laser seed that has $a_0 = .1$ and $\lambda_L = 10\mu$m (blue line). Beam parameters used to generate this figure are given in the text. (b) Axial E_z vs. ζ at $z = 5$ m for the laser-seeded (blue line) and hard-cut cases (red line) of panel (a).

schematically in Figure 2. Figure 3 a) shows E_z^{max}, the maximal on axis electric field, as a function of propagation distance z for a proton beam hard-cut at $\zeta = \sigma_z\sqrt{\pi/2}$ with no laser (black line). This 'cutting' location was found to maximized E_z^{max} for these parameters. Also shown is E_z^{max} vs. z for the 'full' proton beam with a laser seed that has $a_0 = .1$ and $\lambda_L = 10$ μm (blue line). This figure demonstrates that the peak E_z^{max} value achieved from each seed are comparable. Figure 3 b) shows the axial E_z vs. ζ at $z = 5$ m for the laser-seeded (blue line) and hard-cut cases (red line) of Figure 3 a).

CONCLUSION

In summary, we have shown that a laser pulse can be used to efficiently seed the MI within an SPS-LHC proton beam, which is the first proposed experimentally feasible seeding method. We found that a CO_2 laser is the most attractive candidate to seed the MI since it can produce a stronger perturbation throughout the proton bunch without creating signifnicant levels of secondary and tertiary ionization in the Cesium plasma. In order to efficiently seed the MI, the laser's wakefield must exert a force that produces a large, radially inward momentum in regions of the proton beam separated by the plasma wavelength, which leads to the compression of the proton beam in these regions. Finally, we demonstrated that a laser pulse with non-stringent parameters seeds the MI with similar strength to that of the previously proposed hard-cut seeding method.

ACKNOWLEDGMENTS

This work was supported by the US DOE grant DE-FG02-05ER54840.

REFERENCES

1. A. Pukhov and J. Meyer-ter Vehn, Appl. Phys. B 74, 355 (2002); J. Faure et al., Nature (London) 431, 541 (2004); C. G. R. Geddes et al., ibid. 431, 538 (2004); S. P. D. Mangles et al., ibid. 431, 535 (2004); W. P. Leemans et al., Nature Phys. 2, 696 (2006); S. Kneip et al., Phys. Rev. Lett. 103, 035002 (2009); I. Blumenfeld et al., Nature (London) 445, 741 (2007).
2. E. Esarey, P. Sprangle, J. Krall, and A. Ting, IEEE Trans.Plasma Sci. 24, 252 (1996).
3. A. Caldwell, K. Lotov, A. Pukhov, and F. Simon, Nature Phys. 5, 363 (2009); K. V. Lotov, Phys. Rev. ST Accel. Beams 13, 041301 (2010).
4. E. Esarey, J. Krall, and P. Sprangle, Phys. Rev. Lett. 72, 2887 (1994).
5. N. Kumar, A. Pukhov, K. Lotov, Phys. Rev. Lett. 104, 255003 (2010).
6. Ya. B. Fainberg, V. D. Shapiro, and V. I. Shevchenko, Sov. Phys. JETP 30, 528 (1970) Zh. Eksp. Teor. Fiz. 57,966 (1969); M. Lampe and P. Sprangle, Phys. Fluids 18, 475 (1975); M. E. Dieckmann, B. Eliasson, P. K. Shukla, N. J. Sir-combe, and R. O. Dendy, Plasma Phys. Controlled Fusion 48, B303 (2006).
7. E. W. Weibel, Phys. Rev. Lett. 2, 83 (1959); R. L. Morse and C. W. Nielson, Phys. Fluids 14, 830 (1971); R. Lee and M. Lampe, Phys. Rev. Lett. 31, 1390 (1973); R. C. Davidson, D. A. Hammer, I. Haber, and C. E. Wagner, Phys. Fluids 15, 317 (1972); C. Siemon, V. Khudik, G. Shvets, Phys. Plasmas 18, 103109 (2011)
8. E. Esarey, J. Krall, and P. Sprangle, Phys. Rev. Lett. 72, 2887 (1994); D. H. Whittum, Phys. Fluids B 5, 4432 (1993).
9. R. Keinigs and M. E. Jones, Phys. Fluids 30, 252 (1987).
10. M.V. Ammosov, N.B. Delone, and V.P. Krainov, Sov. Phys. JETP 64, 6 (1970)
11. K.V.Lotov, Controlled self-modulation of high energy beams in a plasma, Phys. Plasmas, 18, 024501 (2011).